Fermilab Library
0 1160 0033480 9

IP-BBSR-94-9

IP/BBSR/94-9
March'94

APR

Origin Of Incommensurate Structure in Solids[1]

S.B.Ota
Institute of Physics, Sachivalaya Marg
Bhubaneswar 751005.

2S

NAME | IDNO | REG.

Abstract:

Incommensurate lattice structure is observed in several metals and insulators. Various physical mechanisms leading to incommensurate phase have been suggested, which are reviewed here. Among these, the Fermi surface mechanism has been successful in the case of metals. The origin of incommensurate phase in insulators has been explained by the interacting components mechanism. Recent experiments on Cupric Oxide has examined the validity of this phenomenological theory for magnetic insulators, which was originally worked out for nonmagnetic insulators. Among the microscopic models, the axial next-nearest- neighbor Ising model and the Frank and Van der Merwe model describe how competing interaction lead to incommensurate structure. In this review several physical systems have been discussed in the context of these mechanisms.
PACS numbers: 05.70.Fh, 64.60.-i, 61.

[1]Invited talk presented in the DAE Solid State Physics Symposium, Bhabha Atomic Research Centre, Bombay, December 27-31, 1993.

1.Introduction:

The incommensurate structure in solids has attracted extensive theoretical and experimental study during the last several decades.[1] The incommensurate structure corresponds to a lattice modulation whose period is an irrational fraction of the lattice periodicity. The lattice therefore, lacks translational periodicity while retaining the long range order. The modulation can be of several types. Such as involving displacements, occupation probability of given atoms, or mutually incommensurate basic structures. The x-ray diffraction from such solids are sharp but has additional reflections called 'satellite reflections' along with the main reflections. The indexing of the diffraction pattern from incommensurate solids requires more than the usual three-integer indices. When considered in the context of a phase transition, the crystalline solid undergoes a transition to an incommensurate phase as the temperature is lowered. The amplitude of the incommensurate modulation grows with the decrease in temperature. In some cases the incommensurate wave vector is temperature dependent. The incommensurate phase sometimes undergoes a further transition to a commensurate phase as the temperature is lowered.

There have been great deal of interest in understanding the mechanism leading to incommensurate structure in solids. Among these, the Fermi surface mechanism, the interacting components mechanism (ICM), the axial next-nearest-neighbor Ising (ANNNI) model and the Frank and Van der Merwe (FVdM) model are notable. In the case of metals the Fermi

surface mechanism has been successful. The mechanism is however, not so clear in the case of insulators. The ICM is based on the phenomenological Landau theory and has been used to explain the incommensurate structure in insulators. The ANNNI model describes how competing interactions lead to modulated structures. It has been used to understand the incommensurate structure in some two-state systems. Incommensurate structure is also observed in rare gas monolayers adsorbed on a substrate. This is well accounted for by the FVdM model. In the following sections, several physical systems are discussed in the context of these mechanisms.

2.The Fermi Surface Mechanism:

Some metals with low dimensional feature such as organic conductors, undergo phase transition commonly known as charge density wave (CDW) or Peierls transition.[2,3] The origin of the CDW transition has been attributed as due to the Fermi surface instability involving electron-phonon interaction. The possibility of such an instability was noted by Peierls[4] and later studied by others.[5-9] The origin of the instability can be understood from the susceptibility of the electron-gas system ($\chi(q)$):

$$\chi(q) = \sum_k \left(\frac{f_k - f_{k+q}}{\epsilon_k - \epsilon_{k+q}}\right). \tag{1}$$

Here, f_k is the Fermi function and ϵ_k is the single particle electron energies. In Fig.1, $\chi(q)$ is displayed as a function of wave vector q for one, two and three dimensional electron gas at $T = 0$. It is seen that $\chi(q)$ diverges at

twice the Fermi wave vector $2k_F$ for one dimensional system. This anomaly is less pronounced in two dimensions. It is practically absent in three dimensional systems. At finite temperatures, these anomalies are smeared out. Such anomaly can also arise in 3D systems in the presence of one-dimensional feature. In such a situation, the Fermi surface is nested (i.e., there is a large region of k-space with small energy difference $\epsilon_k - \epsilon_{k+q}$). This anomaly produces a softening of the phonon dispersion at $q = 2k_F$, which leads to a transition at $T = T_{IC}$. Below T_{IC} a permanent lattice distortion occurs with wave vector $2k_F$. In the CDW state, the electronic spectrum is also altered with the presence of an energy gap at $\pm k_F$, which lowers the energy of all the occupied states. For finite temperatures, in the CDW state, the thermally excited electrons screen the electron-phonon interaction which reduces the energy gap self consistently. Therefore, the extent of distortion increases as the temperature is lowered below T_{IC}. It was noted by Peierls that normal metallic conduction would not occur in the low-temperature phase. Instead the material is expected to behave like a semiconductor due to the presence of the energy-gap. Let us consider the case of a CDW distortion of a lattice containing one electron per site. The electron band is then half-filled and the wavelength of the distortion is $2k_F = \pi/a$ where a is the lattice constant. The distortion will hence be commensurate with the lattice periodicity. The incommensurate phase is therefore observed in this elementary case, when the ratio of the number of electrons to the number of sites is not a rational ratio.

Most of the interesting organic conductors are based on the

tetracyanoquinodimethane (TCNQ) molecule. Among these, tetrathiofulvalinium tetracyanoquinodimethane (TTF-TCNQ) has been studied extensively. These are planar molecules (Fig.2a), with electron donor and acceptor properties associated with TTF and TCNQ, respectively. In the solid state, chains of TTF molecule and chains of TCNQ molecule are arranged in the $b-c$ plane with $b-$axis as the stacking direction (Fig.2b). The structure of the high temperature phase is monoclinic. The electrical conductivity is highly anisotropic, with maximum conductivity occuring along the $b-$axis. This indicates that TTF-TCNQ is a quasi-one-dimensional conductor, with electrons confined to be on individual chains. The low temperature electrical conductivity parallel to the $b-$axis undergoes sharp drops at 54 K and 38 K, because of structural transitions involving CDW. Direct evidence of a CDW transition in TTF-TCNQ was first obtained by Denoyer et al[10] by x-ray scattering. Subsequently Kagoshima et al[11] confirmed the presence of a CDW wavevector in this compound. The development of the CDW distortion was studied in the neutron scattering measurements on deuterated TTF-TCNQ single crystal by Comes et al.[12] They observed two structural transformations at 38 K and at 54 K. Below the first order transition at 38K the modulation wave vector of the incommensurate phase is given by $0.295b^*$. The modulation period in the $a-$direction becomes incommensurate at 38K and the corresponding wave vector shows an abrupt increase from its low temperature value of 1/4 and then gradually increases with increasing temperature to 1/2 near 51 K. Subsequently, another transition has been observed at 49 K in the neutron scattering

measurements by Ellenson et al.[13] This additional transition was predicted by Bak and Emery[14] on theoretical grounds as due to the interaction between the orderings in the TTF and TCNQ chains. A comprehensive survey of the experimental work on TTF-TCNQ can be found in the review by Toombs[2].

3.The Interacting Components Mechanism (ICM):

The interaction of two ordering modes is thought to be one of the physical mechanisms giving rise to incommensurate structures in insulators.[15] This viewpoint has been put in a very general phenomenological framework by Heine and McConnell using the two component Landau theory.[16,17] The theory is based on the existence of two transformation modes, which interact under certain conditions. These transformation modes are denoted as the main (ψ) and the subsidiary (ϕ) modes. The transformation modes ψ and ϕ can in general, represent two different kinds of modulations with respect to the unmodulated crystal. The symmetries of these transformation modes are different at the symmetry point in reciprocal space so that they cannot interact there, but they become the same and hence interact at incommensurate points near the symmetry point. These two modes ψ and ϕ are in quadrature in order to have energy lowering interaction. The free energy in this theory is given by,

$$G = G_o + \sum_q [A(q)\psi_q^\dagger\psi_q + H(q)\psi_q^\dagger\phi_q + H(q)^\dagger\psi_q\phi_q^\dagger + B(q)\phi_q^\dagger\phi_q]. \quad (2)$$

Here, $H(q)$ represents the interaction between these two modes. The commensurate and incommensurate phases correspond to $q = 0$ and $q \neq 0$, respectively. The disordered-to-incommensurate transition is second order in nature and occurs at a temperature T_{IC} which is given by,

$$T_{IC} = T_o + \Delta \quad (3)$$

where,

$$\Delta = [(H_1^2/B_o) - A_2]^2[4a(A_4 + ...)]^{-1} \quad and \quad H_1^2/B_o > A_2. \quad (4)$$

Here, A_2, A_4, H_1, B_o, a are parameters assumed to be temperature independent in the expansion of the coefficients in the free energy expression of Eq.2. T_o is the 'fictitious' transition temperature of the main ordering mode. The incommensurate-to- commensurate transition temperature T_C is obtained by equating the free energies of incommensurate and commensurate phases. The transition at T_C is first order in nature at which ϕ disappears discontinuously. T_C is given by:

$$T_C = T_o - 4.45\Delta. \quad (5)$$

If the ϕ mode is also equally soft as compared to ψ, then the incommensurate structure is seen over a wider temperature range and T_C can be even below absolute zero. The details of the ICM theory can be found in Ref.17.

This theory has been applied sucessfully to $NaNO_2$, which is a nonmagnetic insulator.[18] $NaNO_2$ exhibits incommensurate phase for temperatures between 437K and 438.5K. The low temperature ($T < 437K$) phase is ferroelectric and the high temperature ($T > 438.5K$) phase is paraelectric. The structure of $NaNO_2$ is shown in Fig.3. There are two possible orientations ($\pm b$–direction) of the arrow shaped NO_2^- ions. For temperatures above 438.5K, the NO_2^- ions point either in the b or in the $-b$ direction with equal probability. For temperatures below 437K, the probability of pointing in the b–direction is either 0 or 1. Whereas, the probability varies sinusoidally along the a–axis in the incommensurate phase:

$$p(\bar{r}) = 1/2 + \psi_q \cos(qx). \tag{6}$$

Here q is the incommensurate modulation wavevector and is found to be $q \simeq 0.11a^*$. This corresponds to the main mode of the ICM theory. In the incommensurate phase, there is also a local shear of the unit cell in the b–direction and varing sinusoidally along the a–axis:

$$\epsilon_{xy}(\bar{r}) = \phi_q \sin(qx). \tag{7}$$

This corresponds to the subsidiary mode of the ICM theory. We note that the two modulations given in Eqs.6 and 7 are in quadrature. A detail group theoretical analysis of the incommensurate structure in $NaNO_2$ can be found in Ref.18.

Several recent experiments on Cupric oxide (CuO) has provided additional support to this theory and extended the validity to magnetic insulators.[19] CuO is an exception, both structurally and magnetically among the 3d transition metal monoxides. The crystal structure of CuO is monoclinic unlike the cubic structure of other 3d-transition metal monoxides.[20] The antiferromagnetism in CuO is also distinctly different.[21-23] CuO undergoes a second-order paramagnetic-to-incommensurate antiferromagnetic transition at a temperature T_{IC}=229 K.[21-28] This is followed by a first-order incommensurate-to-commensurate antiferromagnetic transition at a temperature T_C=213 K.[22-29] These two transitions are displayed in the temperature dependence of specific heat (Fig.4).[28] The propagation vector of the incommensurate phase $\bar{q}_i = (0.506, 0, -0.483)$ is temperature independent and goes over discontinuously to the commensurate wave vector $\bar{q}_c = (1/2, 0, -1/2)$ at T_C. Neutron scattering experiments show that in the commensurate antiferromagnetic state below T_C, the spins orient parallel to the b–axis, which represents the easy-axis. The incommensurate antiferromagnetic state is found to have a helical modulation with an elliptical moment envelope.[23]

Recently, the effect of magnetic field on the specific heat of a CuO single crystal was studied.[28] It was found that T_C increases nonlinearly for magnetic field applied parallel to the a– and c–axes. Whereas, a linear reduction of T_C is observed for magnetic field applied parallel to the b–axis. Anisotropy was also observed in the temperature dependence of magnetic

susceptibility.[29] This was explained in the framework of ICM theory as follows. For CuO, the main mode corresponds to the commensurate antiferromagnetic ordering below T_C with the easy-axis parallel to the b–axis and the subsidary mode is assumed to correspond to an antiferromagnetic ordering, with the easy axis nearly perpendicular to the normal of the $a-c$ plane. It was argued that by the application of magnetic field, the individual components can be controlled and T_C is affected in an analogous manner. The anisotropic magnetic field dependence of T_C observed in CuO has provided a major experimental support to the ICM theory.

4.The Axial Next-Nearest-Neighbor Ising (ANNNI) model:

Modulated structure arising due to competing short range interactions was pointed out by Elliot in the context of helicoidal spin configurations in heavy rare-earth metals.[30] The basic idea was later studied in the simplistic ANNNI model,[31,32] which makes use of the discrete two-state spin $S_i = \pm 1$. The Hamiltonian of the 3-dimensional ANNNI model is given by,

$$H = -\frac{1}{2}J_o \sum_{ijj'} S_{i,j}S_{i,j'} - J_1 \sum_{ij} S_{i,j}S_{i+1,j} - J_2 \sum_{ij} S_{i,j}S_{i+2,j} \qquad (8)$$

Here, i and j, j' labels spins in layers perpendicular to the axial direction and nearest-neighbor spins within a layer, respectively. The interaction is ferromagnetic within the plane perpendicular to the axial direction (i.e., $J_o > 0$). There is competing interaction in the axial direction, with

ferromagnetic interaction between the nearest neighbour spins (i.e., $J_1 > 0$) and antiferromagnetic interaction between the next nearest neighbour spins (i.e., $J_2 < 0$). The degree of the competition is determined by the ratio $\kappa = -J_2/J_1$. The Hamiltonian shows a variety of modulated phases depending on the degree of competition. The phase diagram of the ANNNI model on a cubic lattice has been studied in the mean-field approximation.[33–35] Fig.5 displays the phase diagram as a function of the parameter κ. At high temperatures the system shows paramagnetic phase. At zero temperature, the ferromagnetic state switches over to the antiphase state at $\kappa = 1/2$. The modulated commensurate phases are observed between the antiphase state and ferromagnetic state at finite temperatures. The paramagnetic-to- modulated phase boundary is second order in nature, whereas the modulated phases are separated by first order transitions. Above certain temperature, stable incommensurate phases are observed inbetween the commensurate phases (Fig.5).[31,36] The ANNNI model explains the origin of the incommensurate phase in a simplified manner, which can also be applied to nonmagnetic systems.

It is well known that a two state system can be mapped onto an Ising model, often with just short-range interactions. One such example is $NaNO_2$, which exhibits an incommensurate phase ($437K < T < 438.5K$) in between the low temperature ferroelectric phase and the high temperature paraelectric phase. The two possible orientations of the NO_2^- ions (Fig.3) can be described by the Ising spin in a crude approximation. Selke and Duxbury[35] explained the phase diagram of $NaNO_2$ in an electric

field using the ANNNI model.

The best example of the ANNNI model is a system where the Ising variables correspond to magnetic spins such as cerium antimonide. In the case of cerium antimonide the spins are constrained to point along [100] direction due to strong uniaxial spin anisotropy. The ordering is ferromagnetic within the (100) planes. At low temperatures below 17 K, the ferromagnetic planes form modulated structures with wavevector along [100], similar to the phases in ANNNI model.[37-41]

5.The Frank and Van der Merwe (FVdM) Model:

Incommensurate structure has been observed in rare gas monolayers adsorbed on a substrate.[31,42-45] This arises due to the mismatch of periodicities between the substrate and the overlayer. The phenomena is understood on basis of the simplistic model of Frank and Van der Merwe.[46] The Hamiltonian of the one dimensional FVdM model is given by:

$$H = \sum_n [\frac{\alpha}{2}(x_{n+1} - x_n - a_0)^2 + \lambda(1 - \cos\frac{2\pi}{b}x_n)] \qquad (9)$$

where x_n is the position of the nth atom, a_0 is lattice constant of the overlayer, b is the period of the substrate potential. The model exhibits several interesting phases. In the absence of the substrate potential (i.e., $\lambda = 0$), the atoms are arranged with a separation a_0. In general, a_0 is not commensurate with b. The presence of the substrate potential modulates

the overlayer. The atoms tend to move towards the minimum of the potential. When the substrate potential is strong, a commensurate modulation of the overlayer is obtained. The incommensurate structure is observed for intermediate strength of the potential. If the substrate potential is extremely strong compared to the interatomic interaction, then the atoms are distributed randomly among the potential minima. This corresponds to the chaotic structure. The situation is qualitatively different in two or three dimensions. The modulation wavevector as a function of the parameter a_0 show several complex features. For instance, the system can go through an infinite sequence of commensurate phases giving rise to the so called 'devil's staircase'. The phase diagram of the FVdM model bears several resemblances with the phase diagram of the ANNNI model. An account of the similarity can be found in the review by Bak.[31]

The krypton monolayer adsorbed on graphite basal plane has been studied in some detail by low energy electron diffraction[42] and x-ray diffraction.[43-45] The adsorbed krypton gives rise to a hexagonal incommensurate structure under high pressure and low temperature. The hexagonal incommensurate structure is characterized in terms of the deviation from the hexagonal commensurate $(\sqrt{3} \times \sqrt{3})30^\circ$ structure with one krypton atom per three graphite hexagons. The temperature dependence of the incommensurability was found to follow a power law given by $\epsilon = \epsilon_o(1 - T/T_C)^{1/3}$ with a T_C of 97 K.[44] The pressure induced commensurate-to- incommensurate transition was studied by Nielsen et al[45] at 40 K employing D_2 gas as the source of two dimensional spreading

pressure. The transition was observed to be first order. Finally, we note that graphite intercalation compounds constitute a natural extension to three dimensions of the adsorbed rare gas monolayer on graphite.

6.Summary:

We have discussed how incommensurate structure arises in solids. In metals with nested Fermi surface, the length of Fermi wave vector may be incommensurate with respect to the reciprocal lattice vector and by the mechanism of the Peierl's instability the incommensurate phase may result. Several microscopic models have been proposed to explain the incommensurate phase. Among these, the ANNNI model describes how the incommensurate structure arises due to competing short range interactions. This model, though simple, has been used to explain modulated structure in some magnetic systems. The FVdM model describes how competing periodicities can give rise to several phases including the incommensurate phase. The incommensurate structure observed in rare gas monolayers adsorbed on graphite has been understood using this model. In the case of insulators, interaction of two ordering modes can give rise to incommensurate structure. This is described by the interacting components mechanism. Being of phenomenological nature based on the Landau theory of phase transition, this provides a sound understanding of the origin of incommensurate structure in insulators. The recent study of the anisotropic magnetic field dependence of incommensurate-to- commensurate transition in CuO, has provided additional support to the ICM-theory. This

observation should invoke further theoretical investigations especially in the context of magnetic insulators.

Acknowledgements:

The author thanks Prof.E.Gmelin and Dr.W.Kress for helpful discussions and remarks.

References:

1) T.Janssen and A.Janner, Advances in Physics 36, 519 (1987).

2) G.A.Toombs, Phys.Rep. 40, 181 (1978).

3) A.J.Berlinsky, Rep.Prog.Phys. 42, 1243 (1979).

4) R.E.Peierls, Quantum Theory of Solids, (Oxford University, London, 1955).

5) H.Fröhlich, Proc.Roy.Soc. London A223, 296 (1954).

6) C.G.Kuper, Proc.Roy.Soc. London A227, 214 (1955).

7) A.W.Overhauser, Phys.Rev.Lett. 4, 462 (1960).

8) J.Bardeen, Solid St. Commun. 13, 357 (1973).

9) P.A.Lee, T.M.Rice and P.W.Anderson, Phys. Rev. Lett. 31, 462 (1973).

10) F.Denoyer, F.Comes, A.F.Garito and A.J.Heeger, Phys. Rev. Lett. 35, 445 (1975).

11) S.Kagoshima, H.Anzai, K.Kajimura and T.Ishiguro, J.Phys.Soc.Japan 39, 1143 (1975).

12) R.Comes et al, Phys.Rev.Lett. 35, 1518 (1975).

13) W.D.Ellenson et al, Solid St. Commun. 20, 53 (1976).

14) P.Bak and V.J.Emery, Phys. Rev. Lett. 36, 978 (1976).

15) V.Heine, Statics and Dynamics of Nonlinear Systems, Springer Series in Solid-State Sciences, edited by G.Benedek, H.Bilz, and R.Zeyher (Springer-Verlag, Berlin, 1983), vol.47 p-98.

16) V.Heine and J.D.C.McConnell, Phys.Rev.Lett. 46, 1092 (1981).

17) V.Heine and J.D.C.McConnell, J.Phys. C 17, 1199 (1984).

18) V.Heine, R.M.Lynden-Bell, J.D.C. McConnell and I.R. McDonald, Z.Phys.B 56, 229 (1984).

19) E.Gmelin, Indian J. Pure and Appl. Phys. (1992).

20) G.Tunell, E.Posnjak, and C.J.Ksanda, Z.Kristallogr. 90, 120 (1935); S.Asbrink and L.J.Norrby, Acta Crystallogr. B 26, 8 (1970).

21) B.N.Brockhouse, Phys.Rev. 94, 781 (1954).

22) B.X.Yang, J.M.Tranquada, and G.Shirane, Phys.Rev.B 39, 174 (1988); B.X.Yang et al., Phys.Rev.B 39, 4343 (1989).

23) J.B.Forsyth, P.J.Brown, and B.M.Wanklyn, J.Phys.C 21, 2917 (1988); P.J.Brown et al., J.Phys.:Condens. Matter 3, 4281 (1991).

24) J.W.Loram, K.A.Mirza, C.P.Joyce, and A.J.Osborne, Europhys. Lett. 8, 263 (1989).

25) E.Gmelin, U.Köbler, W.Brill, T.Chattopadhyay and V.S.Sastry, Bull.Mater.Sci. 14, 117 (1991).

26) A.Junod et al., J.Phys.:Condens. Matter 1, 8021 (1989).

27) E.Gmelin, W.Brill, and T.Chattopadhyay, Thermochim. Acta 160, 43 (1990).

28) S.B.Ota and E.Gmelin, Phys.Rev.B 46, 11632 (1992).

29) U.Köbler and T.Chattopadhyay, Z.Phys.B 82, 383 (1991).

30) R.J.Elliott, Phys.Rev. 124, 346 (1961).

31) P.Bak, Rep.Prog.Phys. 45, 587 (1982).

32) J.Yeomans, Solid State Physics, edited by H.Ehrenreich and D.Turnbull, (Academic, New York 1988), vol.41 p-151.

33) P.Bak and J.von Boehm, Phys.Rev.B 21, 5297 (1980).

34) P.M.Duxbury and W.Selke, J.Phys.A 16, L741 (1983).

35) W.Selke and P.M.Duxbury, Z.Phys.B 57, 49 (1984).
36) M.H.Jensen and P.Bak, Phys.Rev.B 27, 6853 (1983).
37) B.Lebech, K.Clausen and O.Vogt, J.Phys.C 13, 1725 (1980).
38) P.Fischer, B.Lebech, G.Meier, B.D.Rainford and O.Vogt, J.Phys.C 11, 345 (1978).
39) G.Meier, P.Fischer, W.Halg, B.Lebech, B.D.Rainford and O.Vogt, J.Phys.C 11, 1173 (1978).
40) J.Rossat-Mignod, P.Burlet, J.Villain, H.Bartholin, T.S.Wang, D.Florence, and O.Vogt, Phys.Rev.B 16, 440 (1977).
41) J.Rossat-Mignod, P.Burlet, H.Bartholin, O.Vogt and R.Lagnier, J.Phys.C 13, 6381 (1980).
42) M.D.Chinn and S.C.Fain, Jr., Phys.Rev.Lett. 39, 146 (1977).
43) P.W.Stephens, P.Heiney, R.J.Birgeneau and P.M.Horn, Phy.Rev.Lett. 43, 47 (1979).
44) D.E.Moncton et al., Phys.Rev.Lett. 46, 1533 (1981).
45) M.Nielsen, J.Als-Nielsen, J.Bohr and J.P.McTague, Phys.Rev.Lett. 47, 582 (1981).
46) F.C.Frank and J.H. van der Merwe, Proc. Roy. Soc. London A198, 205 and 216 (1949).

Figure Captions:

Figure.1 The zero temperature susceptibility of the free electron Fermi gas as a function of the wave vector q in one, two and three dimensions. The susceptibility diverges at twice the Fermi wave vector in one dimensional system.

Figure.2(a) The tetrathiofulvalinium (TTF) and tetracyanoquinodimethane (TCNQ) molecule. (b) The projection of TTF-TCNQ structure in the $a-c$ plane. The molecules shown with bold lines are $b/2$ above the $a-c$ plane. The chains of TTF and TCNQ molecules are arranged in the $b-c$ plane with $b-$axis as the stacking direction.

Figure.3 The projection of $NaNO_2$ structure in the $b-c$ plane. The atoms shown with light lines are $a/2$ above the $b-c$ plane. There are two possible orientations ($\pm b-$direction) of the arrow shaped NO_2^- ions. The probability of pointing in the $b-$direction is 1/2 in the high temperature phase, 1 (or 0) in the low temperature phase and varies sinusoidally along the $a-$direction in the incommensurate phase.

Figure.4 The temperature dependence of specific heat of a CuO single crystal. The anomaly at 228.5K corresponds to the second-order paramagnetic-to-incommensurate antiferromagnetic transition. The anomaly at 212.6K corresponds to the first-order incommensurate-to-commensurate antiferromagnetic transition.

Fig. 1

Figure.5 The phase diagram of the cubic ANNNI model in the mean field approximation. The main commensurate phases are indicated by the conventional notation. For example < 223 > represents ... ↑↑↓↓↑↑↑ .... The antiphase state corresponds to ... ↑↑↓↓↑↑ .... The incommensurate phases are found between the commensurate phases above the dashed line.

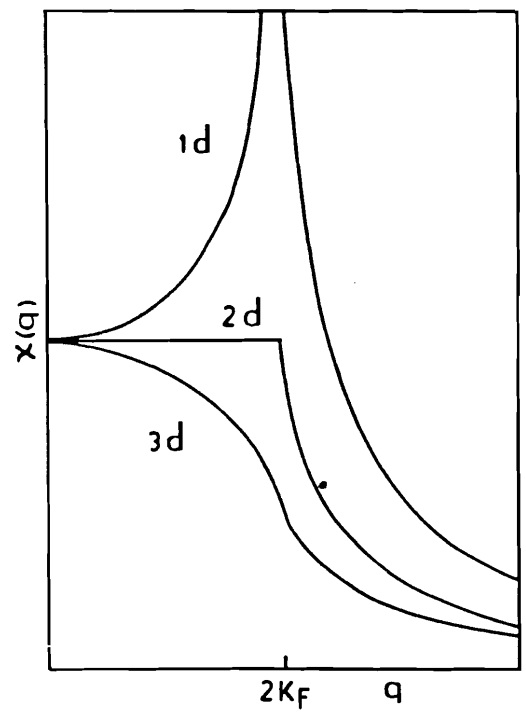

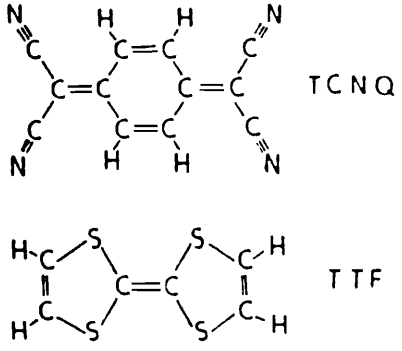

(a)

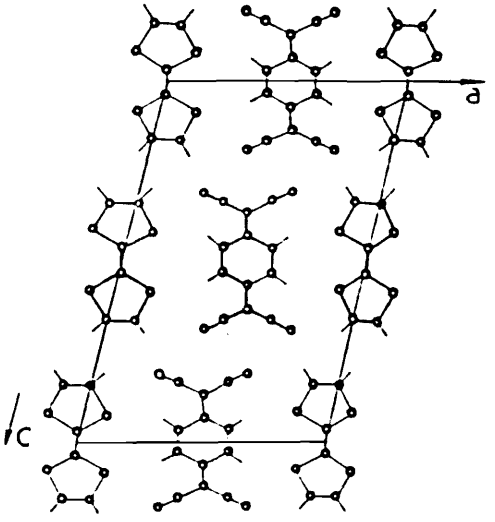

(b)

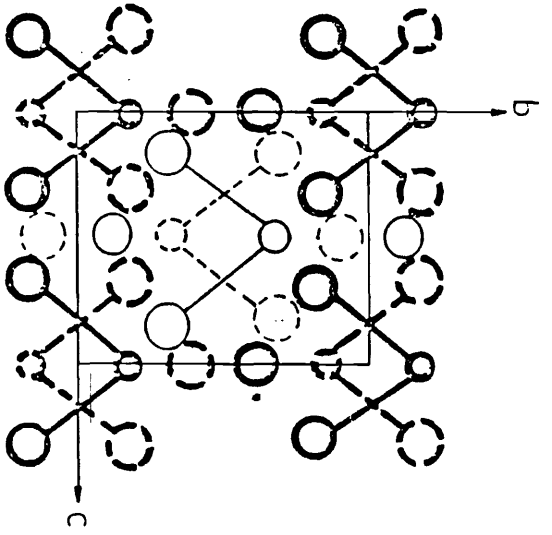

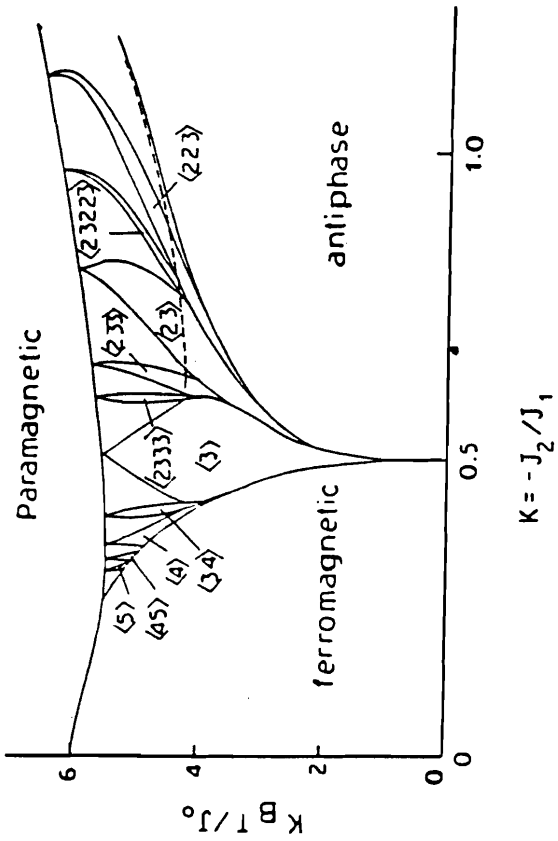
Paramagnetic
ferromagnetic
antiphase
K = -J2/J1
KBT/J0
0
0.5
1.0
2
4
6
(5)
(45)
(4)
(34)
(3)
(2333)
(233)
(23)
(2322)
(223)

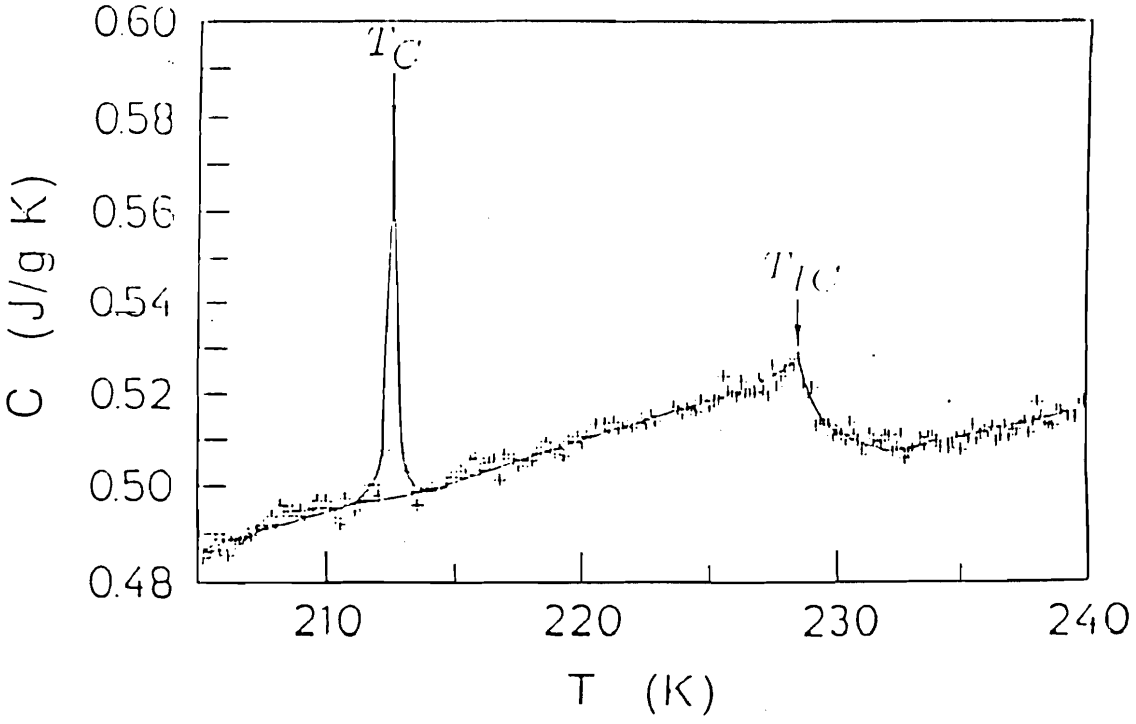
C (J/g K)
T (K)
0.60
0.58
0.56
0.54
0.52
0.50
0.48
210
220
230
240
TC
TIC